Original paper

End-to-end test and MOSFET *in vivo* skin dosimetry for ^{192}Ir high-dose-rate brachytherapy of chronic psoriasis

Lalida Tuntipumiamorn, MSc, Pitchayut Nakkrasae, MSc, Sansanee Kongkum, BSc, Pittaya Dankulchai, MD

Division of Radiation Oncology, Department of Radiology, Faculty of Medicine, Siriraj Hospital, Mahidol University, Bangkok, Thailand

Abstract

Purpose: This study was performed using end-to-end testing and real-time *in vivo* skin dose measurements, using metal oxide semiconductor field effect transistor (MOSFET) dosimeters on our first chronic psoriasis patient treated with iridium-192 (^{192}Ir) high-dose-rate (HDR) brachytherapy (BT).

Material and methods: Treatment delivery was planned with the prescription dose of 1.8 Gy to a 3 mm depth for 12 fractions, using our custom-fabricated surface mold and Varian soft catheters. The optimal technique to provide an adequate and acceptable skin dose as well as its feasibility were evaluated by an end-to-end exercise using a perspex finger phantom. The accuracy and reliability of MOSFET dose measurement was explored with a thermoluminescence dosimetry (TLD) before being used *in vivo* to monitor skin doses during treatment delivery for each BT fraction.

Results: Using custom-made surface mold (2.4 mm Med-Tec thermoplastic mask for hand fixation and 5 applicators attached to each finger for dose delivery), the optimal skin dose on the phantom was obtained without the need for additional bolus to increase thickness of applicator. We acquired mean skin doses at different skin depths from various dose-volume parameters of no-bolus and 3 mm-added bolus plans. They were 125% and 110% (1 mm), 120% and 108% (2 mm), and 114% and 106% (3 mm), respectively. There was excellent agreement between MOSFET and TLD for ^{192}Ir HDR-BT within ±3% (mean 2.65%, SD = 2.05%). With no energy correction, MOSFET overestimated the Acuros BV surface doses by up to 7% in the phantom study and in the clinical case.

Conclusions: We demonstrated achievable HDR-BT for our first case of nail bed psoriasis. The end-to-end exercise was an efficient methodology to evaluate new feasibility for this technique. Real-time dose monitoring using MOSFET was an effective and reliable tool to ensure treatment quality and patient safety.

Purpose

A recent survey of current practice patterns revealed that skin surface brachytherapy (BT) is the preferred treatment option for non-melanoma skin cancers [1]. Compared to external beam radiotherapy, BT provides superior dosimetric outcomes for superficial application within any surface, including very irregular surfaces and, in particular, tumors located within curved surfaces [2]. Absorbed dose simulations in near-surface regions have also confirmed that high-dose-rate (HDR) iridium-192 (^{192}Ir) is an optimal radiation source for skin lesions, especially for the treatment of conditions with bone located directly beneath the skin [3,4]. Besides skin cancers, satisfactory results of the use of ^{192}Ir HDR-BT with chronic dermatitis, such as palmoplantar pustulosis on feet or ankles, have been presented [5]. The role of HDR-BT in stimulating T-cells, a significant component

of the inflammatory infiltrate of psoriatic lesions, in order to increase the immune response has also recently been demonstrated [6]. In that study, HDR-BT was found to be well-tolerated, with adequate disease control. Using the same approach employed with skin cancers or superficial lesions, it is important that a known radiation dose from ^{192}Ir HDR-BT is released into a patient's skin when an organ at risk is considered or if the skin is included in the target volume. Undesirable results, such as radiation dermatitis, have been found to be correlated with skin dose. Therefore, the accurate prediction of the skin dose during treatment planning is clinically relevant, but most of treatment planning systems (TPSs) have limitations in predicting the dose within several millimeters of the body surface. To ensure that intended treatments are accurately performed, the American Brachytherapy Society working group suggested an end-to-end test case

using a phantom, especially with patients undergoing complex BT [7]. The use of *in vivo* dosimetry to verify doses during the whole chain of treatment preparation and delivery has also been recommended by several professional organizations [8,9,10]. Online *in vivo* dosimeters, such as diodes and metal oxide semiconductor field effect transistors (MOSFETs), have been introduced for use in radiotherapy. In the case of MOSFETs, their small physical size, easy to operate, and reproducible and reliable measurements, have helped them to gain popularity for use in external beam radiotherapy with both photon and electron treatments [11,12,13,14,15]. A number of studies have also investigated the application of *in vivo* dosimetry for high-dose and low-dose-rate BT [16,17,18,19,20].

In this study, ^{192}Ir HDR-BT was used for our first psoriatic nail bed patient. Its technical feasibility was evaluated through an end-to-end test on a finger phantom. The actual doses applied with the prescribed technique were monitored using MOSFET *in vivo* dose verification.

Material and methods

Treatment simulation and planning

A 62-year-old female patient who presented with psoriatic nail beds on 9 fingers of both hands was planned to receive ^{192}Ir HDR-BT, with a prescribed dose of 21.6 Gy in 12 fractions (1.8 Gy per fraction) to clinical target volume. Considering the curved surface of fingers, the dose was planned to be delivered through a custom mold surface applicator with flexible plastic catheters and a VariSource iX HDR afterloader (Varian Medical Systems, Palo Alto, CA, USA). A research by Buzurovic *et al.* described the treatment preparation [6], but in our study, it was modified in accordance with our resources. Firstly, the area of the clinical target was localized on each finger and then, the patient's hand was positioned and immobilized with a 2.4 mm Med-Tec thermoplastic mask. Five plastic catheters, one for each finger, were mounted in a position needed to deliver a whole dose coverage to the target area. To ensure the applicators were positioned in a highly reproducible setup, an additional small pieces of Med-Tec

mask were used to secure them on the mask (Figure 1). For the treatment simulation, a 1.5 mm slice thickness was used for CT image acquisitions (GE BrightSpeed; GE Medical Systems, Milwaukee, WI), and all images were exported to the BT planning system (BrachyVision, version 13.6, Varian Medical Systems, Palo Alto, CA, USA). The clinical target volume with a depth of 3 mm was contoured by a radiation oncologist. A medical physicist performed the catheter reconstruction (45 catheters in total) and generated a 3D-based treatment plan (using an Acuros BV [ABV], compliant with BrachyVision). A dosimetric goal of 100% isodose coverage at a depth of 3 mm under the surface, and kept at a 125% line off the skin to spare stem cells and vasculature [6,21] was established for the planning optimization.

Phantom study

Using superficial HDR-BT for the patient's nail beds was a complex procedure for our team, since we had no previous experience and many manual steps were involved. With the aim of delivering an adequate and optimal skin dose to the patient, the technical feasibility of the therapy, based on our resources and experiences was evaluated by an end-to-end exercise on the entire treatment chain, which included the applicator placement, immobilization, imaging, planning, and execution of the plan by the afterloader, using a custom-made, perspex, finger phantom. The optimal surface doses from two different treatment plans (using no-bolus and 3 mm-added bolus above the skin surface), which were generated with a prescription dose (PD) of 1.8 Gy at a depth of 3 mm, were also investigated. The accuracy of the planned skin doses obtained from the ABV algorithm were well verified with the MOSFET (TN-502RD) detectors at 5 locations of the phantom surface, as illustrated in Figure 2.

Accuracy and reliability of MOSFET for ^{192}Ir high-dose-rate brachytherapy

Measurements of the skin doses from ^{192}Ir HDR-BT were made using dual-bias TN-502RD MOSFET of stan-

Fig. 1. The patient with thickening and crumbling of the nails was prepared for the custom-made surface mold by using a 2.4 mm Med-Tec thermoplastic mask, with 5 flexible plastic applicators on each finger. All catheters were secured with small pieces of Med-Tec mask
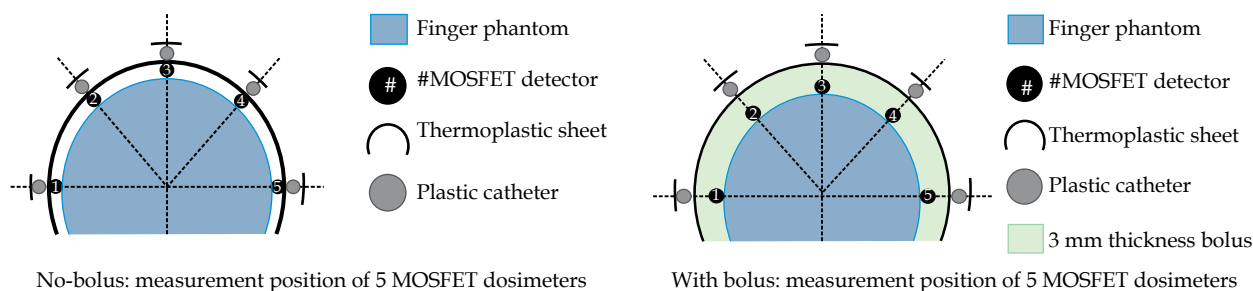
Fig. 2. The measuring points of the MOSFET detectors on the finger phantom for no-bolus and 3 mm-added bolus technique, to assess the optimal skin dose and to verify the accuracy of calculated skin doses obtained from the ABV algorithm

dard sensitivity and an online wireless readout system for 5 detectors (Best Medical Canada, Ottawa, Ontario, Canada). All MOSFET characteristics (linearity, reproducibility, dose-rate, and angular dependence) had previously been examined, and all dosimeters were calibrated with an external beam, 6 MV X-ray photon from a linear accelerator (TrueBeam, Varian Medical Systems, Palo Alto, CA, USA). Using the same setup, an indirect method to determine the energy correction of MOSFET for ^{192}Ir was undertaken. All MOSFET readings from 8 locations of the in-house phantom were compared to the readings from LiF (Mg, Ti) thermoluminescence dosimeters (TLD-100, Thermo Fisher Scientific Inc., Waltham, MA), which had been calibrated to a ^{60}Co γ ray. The in-house wax phantom was embedded with tandem and ring applicators, and used Gammex RMI compact and sponge bone material to represent tissue inhomogeneity, as illustrated in Figure 3. Then, with an ABV calculation algorithm, the treatment planning with a prescription dose to point A of 7 Gy was performed to generate pear-shaped isodose distributions. The delivered doses from the VariSource iX afterloader were subsequently measured and repeated 3 times with both detectors.

Clinical real-time dose monitoring

For every treatment fraction, a single MOSFET detector was attached to the patient's skin at the middle of the treated finger, with the epoxy side facing the source (Figure 4). The setup accuracy and reproducibility were inspected by the team, and all catheters were connect-

ed to the transfer tube for dose delivery. The length of treatment for each applicator (the source indexer length) had previously been measured using a Varian measurement ruler, and the source positioning accuracy was verified using an autoradiograph technique. After the setup phase was completed, the treatment plan was executed, and the monitoring of the actual doses given during the treatment delivery was performed by the MOSFET detector *in vivo* dosimetry.

Results

MOSFET accuracy and reliability for high-dose-rate brachytherapy

With an irradiated dose of 0.5-20 Gy to the MOSFET, an excellent dose linearity ($R^2 = 0.9997$) was achieved. The calibration factors with 6 MV X-ray photon were in the range of 0.868-0.903 in cGy/mV. Table 1 presents the results of the ABV calculated skin doses as well as the MOSFET and TLD measured doses at 8 locations in our in-house phantom. The energy response factor 1.03 of ^{192}Ir relative to ^{60}Co, which has been reported by a few studies was used to correct the energy dependence of all of the TLD readings [22,23,24]. At the same measurement point, the uncorrected MOSFET reading was compared to the corrected TLD, and the mean ratio of both readings (MOSFET/TLD) was found to be 1.03 (range, 0.99-1.05); this beam quality difference correction factor was used for all MOSFET readings in this study. Both the TLDs and MOSFETs overestimated the ABV planned dose,
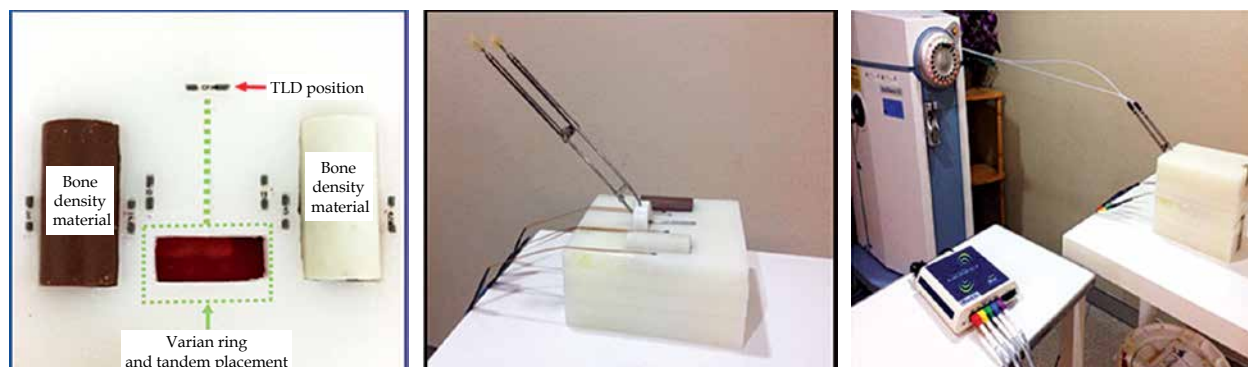

Fig. 3. The in-house wax phantom embedded with tandem and ring applicators, and Gammex RMI compact and sponge bone material to represent tissue inhomogeneity. They were designed to measure the doses from the VariSource iX afterloader at 8 different phantom cavities, using TLD-100 and TN-502RD MOSFET dosimeters
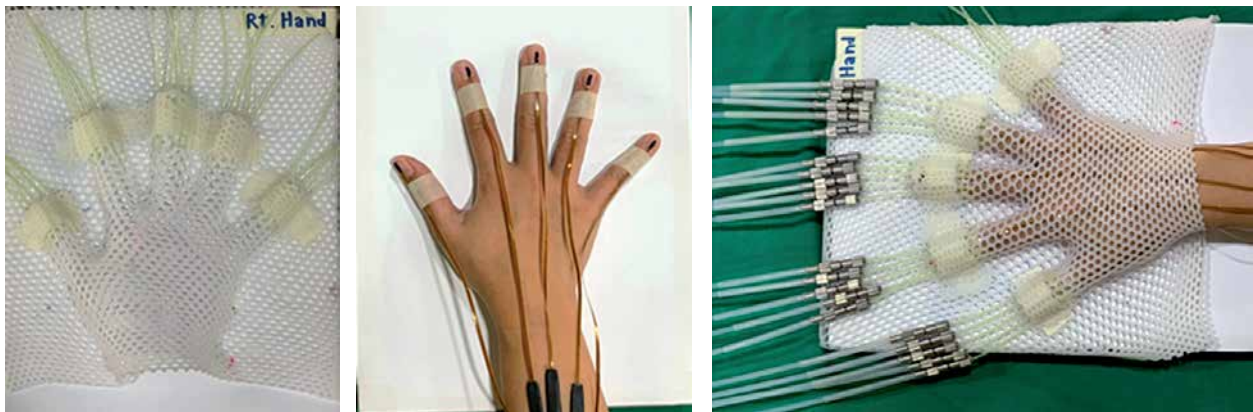
Fig. 4. An individual MOSFET TN-502RD detector was attached on the middle of patient's nail, with the epoxy side facing the source. A custom-made mold was subsequently placed above the patient's hand and checked for its setup accuracy before the catheters were connected to the afterloader transfer tube for treatment delivery

with a mean ratio of TLD/ABV of 1.03 (range, 1.00-1.06). A similar result for MOSFET$_{corrected for beam energy}$/ABV of 1.03 (range, 0.99-1.07) was demonstrated.

Determination of optimal technique

Figure 5 illustrate the isodose planning and dose-volume histogram for without and with 3 mm bolus technique. The mean doses for the skin volumes at depths of 1, 2, and 3 mm for the no-bolus plan were 125%, 120%, and 114%, respectively, compared with 110% (1 mm), 108% (2 mm), and 106% (3 mm) for the technique of adding bolus to the skin. The uncorrected MOSFET-measured doses in the finger phantom are shown in Table 2 as well as the doses at 5 locations between 2.27-2.59 Gy (126-144% of PD) for without bolus, and 2.09-2.26 Gy (116-125% of PD) for 3 mm bolus technique. Based on these findings, the adequate and optimal skin dose for the patient's lesion was seen from the no-added bolus technique. As to the accuracy of the ABV in surface dose predictions, the agreement between the planned doses and the MOSFETs was within ±3% for points at the flat surface for the no-bolus technique, while a difference of more than 10% was observed at the 2 measuring points located at the distal end of the finger (point numbers 1 and 5 in Figure 2). Turning to the added-bolus plan, all of the MOSFET-measured skin doses overestimated the calculated dose by about 6-7% for all points. The observed deviation was predicted to be from the displacement of the MOSFET detector in the high-dose gradient field of BT as well as from the energy dependence.

MOSFET real-time in vivo dose measurements

Table 3 presents MOSFET real-time *in vivo* skin dose verifications for the right (5 fingers) and left (4 fingers) hands for all 12 treatment fractions. All presented readings were corrected for their energy response with ^{192}Ir, using the correction factor of 1.03 as previously mentioned. From the results, it can be observed that doses measured on the little finger of the right hand for the second and third fractions were higher than the expected doses. Therefore, the responsible oncologist decided to perform re-optimization of planning to obtain a more ap-

Table 1. Results of the doses (Gy) from the ABV calculation algorithm and measured doses from the TLD and MOSFET dosimeters at the various points in the in-house phantom

Point	ABV	MOSFET$_{UNC}$	TLD$_{COR}$	MOSFET$_{UNC}$/TLD$_{COR}$	MOSFET$_{COR}$/ABV	TLD$_{COR}$/ABV
1	6.30	6.46	6.51	0.99	0.99	1.03
2	6.15	6.52	6.42	1.02	1.03	1.04
3	1.73	1.82	1.77	1.03	1.02	1.02
4	8.35	9.19	8.84	1.04	1.07	1.06
5	8.01	8.55	8.38	1.02	1.04	1.05
6	1.72	1.81	1.79	1.01	1.02	1.04
7	9.95	10.58	10.02	1.06	1.03	1.01
8	8.69	9.11	8.70	1.05	1.02	1.00
Mean	6.36	6.75	6.55	1.03	1.03	1.03
SD	3.12	3.34	3.18	0.02	0.02	0.02

UNC – readings were uncorrected for beam quality differences, COR – readings were corrected with the energy response factor for ^{192}Ir
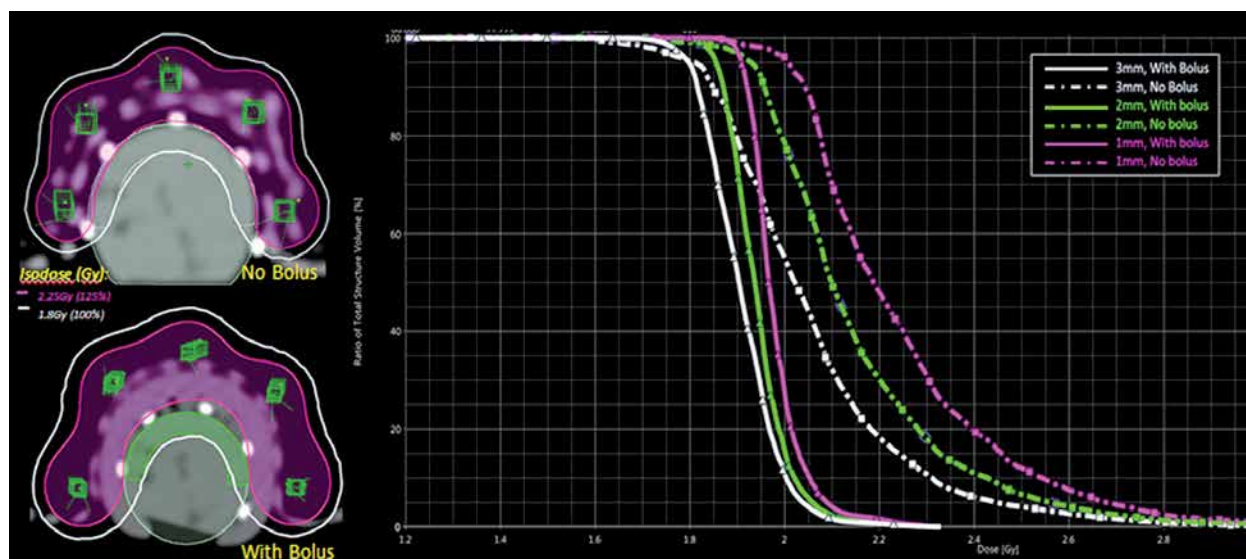
Fig. 5. Generated isodose distribution and dose-volume histogram comparison of the doses and skin volumes at depths of 3 mm, 2 mm, and 1 mm for the no-bolus and with 3 mm bolus technique on the finger phantom

Table 2. Dose readings from the ABV algorithm and MOSFET at 5 points of the finger phantom surface

	Location	Dose (Gy)		
		ABV	MOSFET$_{UNC}$	% dose difference
No bolus	1	2.08	2.34	12.41
	2	2.62	2.66	1.43
	3	2.49	2.44	−1.96
	4	2.50	2.43	−2.77
	5	2.41	2.67	10.69
Added bolus	1	2.19	2.33	6.29
	2	2.03	2.15	6.04
	3	2.15	2.29	6.35
	4	2.04	2.17	6.53
	5	2.05	2.17	6.01

% dose difference = (measured dose – calculated dose)/measured dose * 100

propriate treatment dose for subsequent fractions. After the treatment course was completed, all measured doses were averaged, and excellent agreements (within 5%) were exhibited between the actual doses given and the expected doses.

Discussion

Brachytherapy modalities for skin lesions are commonly used in daily clinical practice, with commercially designed applicators such as Leipzig, Valencia, and electronic BT [25]. However, there is limited availability of special equipment for skin BT for irregular surfaces, and treatment centers are required to fabricate their own customized surface mold applicators to reach the treatment objectives for specific sites. To ensure the accuracy,

efficacy, and safety of these manually-made applicators, an authorization and quality assurance program is recommended to be conducted before their implementation in clinics. In our study, we used the end-to-end exercise on a finger phantom to check our technical feasibility. The learning experience from the whole process definitely helped us to manage this complex application in a convenient way, meeting the expected compliance.

Regarding the challenges in skin dosimetry, skin doses calculated with the treatment planning system for external beam radiotherapy may be within ±25% accuracy [26,27,28]. As to HDR-BT, the applicator thickness (the source to skin distance) and the accurate predicted skin dose are important variables. Granero *et al.* compared predicted surface doses for skin of AAPM TG-43 and ABV calculation algorithms, and investigated the influ-

Table 3. The patient's actual skin doses received from 12 treatment fractions on both hands (9 fingers), compared with the TPS expected doses

Location	TPS dose (Gy)	Measured dose (Gy)												Avg ±SD	% diff
		F1	F2	F3	F4	F5	F6	F7	F8	F9	F10	F11	F12		
Right hand															
Thumb	2.99	3.18	3.12	3.05	2.81	2.96	3.12	3.27	2.71	3.01	2.75	3.11	2.94	3.00 ±0.17	0.33
Index finger	2.62	2.72	2.83	2.94	2.64	2.64	2.50	2.52	2.54	2.46	2.60	2.51	2.49	2.62 ±0.15	0.15
Middle finger	2.43	2.45	2.54	2.62	2.53	2.55	2.60	2.58	2.44	2.56	2.47	2.60	2.52	2.53 ±0.06	3.95
Ring finger	2.56	2.80	2.74	2.67	2.53	2.48	2.96	2.70	2.78	2.62	2.64	2.62	2.66	2.67 ±0.13	4.26
Little finger	2.94	3.06	3.28	3.49	2.92	2.98	2.86	2.84	3.07	2.83	2.75	2.68	2.52	2.94 ±0.20	0.16
Left hand															
Thumb	2.54	2.84	2.56	3.39	2.66	2.51	2.74	2.05	2.55	2.51	2.03	2.28	2.59	2.56 ±0.36	0.65
Index finger	2.49	2.66	2.61	2.84	2.48	2.57	2.62	2.71	2.67	2.54	2.69	2.48	2.49	2.61 ±0.11	4.66
Ring finger	2.43	2.21	2.36	2.32	2.48	2.08	2.47	2.34	2.27	2.38	2.44	2.53	2.46	2.33 ±0.14	4.25
Little finger	2.33	2.57	2.43	2.47	2.98	2.25	2.35	2.24	2.30	2.39	2.36	2.38	2.40	2.37 ±0.10	1.34

*% diff = % dose difference (measured dose – TPS dose)/measured dose * 100*

ence of adding bolus material over custom-made mold [29]. They concluded that when using TG-43 dose calculation for the superficial mold or when the source is in contact with the skin surface, no added bolus is needed for either ^{60}Co or ^{192}Ir. Furthermore, Boman *et al.* showed the validity of ABV and TG-43 in HDR-BT superficial mold treatments [30]. They demonstrated the importance of model-based dose algorithms, as discussed in TG-186, for dose prediction accuracy. They also demonstrated that ABV algorithm showed large agreement with Monte Carlo calculation (within 2%) for the superficial mold treatment and agreed (within 1.5%) with the film measurements. In addition, their study found that there was no need for bolus material above the treatment catheters for ABV, while a strong impact of additional back scatter material applied above surface molds to the dose distributions was revealed for TG-43. In the present study, the ABV was the available algorithm; therefore, we did not apply any additional back scatter material on the hand mask. With regard to the applicator thickness, most skin BT practice activated dwell points at distances of 2-5 mm from the skin [7]. With our technique, since a 2.4 mm plastic mask is already applied to ensure hand fixation, the need for an additional bolus to increase the applicator thickness is questionable. From our investigation, the no-bolus plan offered both an adequate dose to the prescribed depth as well as an acceptable surface dose, and the mean skin dose at a depth of 1 mm (the dermal layer) presented 125%. This is within the tolerance level reported by the American Brachytherapy Society working group, which stated that in order to avoid undesirable results, the optimal skin dose received from the flaps should be limited to 125%, and to 140% for custom-made molds [7]. Moreover, the mean skin dose presenting as 120% at a depth of 2 mm is a valuable information for treatment planning in cases where treated region pres-

ents with bone beneath the skin. As to the dose difference between the without and with bolus plans, the electron dose contribution from the source, which can penetrate skin up to 2 mm distance was reported by Safigholi *et al.* [21]. Hence, the lower skin dose of about 10-15% from the 3 mm-added bolus plan used in this study should be due to the absorption of secondary electrons, resulting from placing a bolus of adequate thickness on the skin.

Turning to the accuracy of MOSFETs in HDR-BT, many studies characterized their accuracy with TLDs, films, and Monte Carlo calculations, and the results showed all detectors agreement within 3% [31]. In our comparison, the accuracy of MOSFET with TLDs also presented within ±3% (mean, 2.65%; SD, 2.05%). Compared to the TPS dose, overestimated responses of 1.6-7.1% from MOSFETs were found by our investigation, which are similar to the results of a study by Persson *et al.* [32]. Their study showed that the overestimations of MOSFET (uncorrected for energy response) to TPS dose values were 2-7% for the end-to-end measurements in HDR prostate and head and neck implantations. Inaccuracy of the MOSFET detectors (±4%) was reported, and the deviations between the planned and measured dose values were markedly influenced by the tube applicator geometry and the positioning of the patient during irradiation [33].

Difficulty in directly calibrating an HDR ^{192}Ir source due to high-dose gradient field is usually exhibited; therefore, MOSFETs are commonly calibrated using ^{60}Co or a megavoltage source because of their well-established dosimetry. Hence, our study was limited by the lack of published data on the energy response of MOSFET to ^{192}Ir source. In our work, a mean correction factor for MOSFET was 1.03 (range, 0.99-1.06; 1 SD, 0.02), which was derived from the comparison with TLDs and it was applied to all MOSFETs regardless of their individual sensitivity; an uncertainty of about 2% (1 SD) could be

expected. The additional inaccuracy was associated with using TLD for ^{192}Ir energy, which was reported by Roue *et al.* [34]. They reported on a mailed TLD system, which was developed by the BRAPHYQS (the BRAchytherapy PHYsics Quality Assurance System) for a remote dosimetry audit for ^{192}Ir HDR and PDR. The largest component of uncertainty, 2.56% (1SD), from an overall uncertainty of 6.54% (2 SD) was demonstrated from the energy correction factor from ^{60}Co to ^{192}Ir beam. The deviation of ≤ 5% between the TLD and the institute stated dose was suggested to be optimal, and a dose variation ≥ 5% but ≤ 7% was defined as the tolerance level. Nevertheless, with the corrected or uncorrected readings for MOSFET, satisfactory dosimetric outcomes with acceptable accuracy from HDR-BT were presented with our first psoriatic nail bed patient. The results of our *in vivo* dose verification were seen to deviate from the expected doses, with ≤ 5% (0.15-4.66%) with- and ≤ 7% (1.61-7.02%) without the beam energy correction for the MOSFET readings.

Our initial experience with the custom-made applicator employed in this investigation indicated that it can be utilized for patients with a high setup accuracy. Moreover, the simple molding process involves low labor costs, the applicator is easy to set up, and it provides good immobilization and reproducibility.

Conclusions

An achievable HDR-BT application for our first case of psoriasis of the nail bed was demonstrated. The end-to-end exercise on a finger phantom definitely helped us to evaluate the technical feasibility of the whole process before its clinical implementation. Dose monitoring by the MOSFET system proved to be an effective and reliable tool to ensure treatment quality and patient safety.

Acknowledgements

Disclosure

Authors report no conflict of interest.

References

1. Likhacheva AO, Devlin PM, Shirvani SM et al. Skin surface brachytherapy: A survey of contemporary practice patterns. *Brachytherapy* 2017; 16: 223-229.
2. Guinot JL, Rembielak A, Perez-Calatayud J et al. GEC-ESTRO ACROP recommendations in skin brachytherapy. *Radiother Oncol* 2018; 126: 377-385.
3. Moura ES, Zeituni CA, Sakuraba RK et al. Absorbed dose simulations in near-surface regions using high dose rate Iridium-192 sources applied for brachytherapy. *Radiat Phys Chem* 2014; 95: 299-301.
4. Safigholi H, Song WY, Meigooni A. Optimum radiation source for radiation therapy of skin cancer. *J Appl Clin Med Phys* 2015; 16: 219-227.
5. Timerman D, Devlin PM, Nambudiri VE et al. Novel application of high-dose rate brachytherapy for severe, recalcitrant palmoplantar pustulosis. *Clin Exp Dermatol* 2016; 41: 498-501.
6. Buzurovic IM, O'Farrell DA, Bhagwat MS et al. Custom-made micro applicators for high-dose-rate brachytherapy treatment of chronic psoriasis. *J Contemp Brachytherapy* 2017; 9: 263-269.
7. Ouhib Z, Kasper M, Calatayud JP et al. Aspects of dosimetry and clinical practice of skin brachytherapy: The American Brachytherapy Society working group report. *Brachytherapy* 2015; 14: 840-858.
8. International Atomic Energy Agency. Development of procedures for in vivo dosimetry in radiotherapy. Human Health Reports no. 8. IAEA, Vienna 2013.
9. Loof M, Nystrom H, Fiorino C et al. Practical guidelines for the implementation of in vivo dosimetry with diodes in external radiotherapy with photon beams (entrance dose). ESTRO Booklet No 5. European Society for Therapeutic Radiology, Brussels 2001.
10. Van Dam J, Marinello G. Methods for in vivo dosimetry in external radiotherapy. ESTRO Booklet No 1 (2nd ed.). European Society for Therapeutic Radiology, Brussels 2006.
11. Marcié S, Charpiot E, Bensadoun RJ et al. In vivo measurements with MOSFET detectors in oropharynx and nasopharynx intensity modulated radiation therapy. *Int J Radiat Oncol Biol Phys* 2005; 61: 1603-1606.
12. Ramaseshan R, Kohil KS, Zhang TJ et al. Perfomance characteristics of a micro MOSFET as an in-vivo dosimeter in radiation therapy. *Phys Med Biol* 2004; 49: 4031-4048.
13. Ramani R, Russell S, O'Brien P. Clinical dosimetry using MOSFETs. *Int J Radiat Oncol Biol Phys* 1997; 37: 959-964.
14. Gopiraj A, Billimagga RS, Ramasubramanian V. Performance characteristics and commissioning of MOSFET as an in-vivo dosimeter for high energy photon external beam radiation therapy. *Rep Pract Oncol Radiother* 2008; 13: 114-115.
15. Dybek M, Łobodziec W, Kawa-Iwanicka A et al. MOSFET detectors as a tool for the verification of therapeutic doses of electron beams in radiotherapy. *Rep Pract Oncol Radiother* 2005; 10: 301-306.
16. Qi Z, Deng XW, Cao XP et al. A real-time in vivo dosimetric verification method for high-dose rate intracavitary brachytherapy of nasopharyngeal carcinoma. *Med Phys* 2012; 39: 6757-6763.
17. Qi ZY, Deng XW, Huang SM et al. Verification of the plan dosimetry for high dose rate brachytherapy using metal-oxide semiconductor field effect transistor detectors. *Med Phys* 2007; 34: 2007-2013.
18. Kwan IS, Wilkinson D, Cutajar D et al. The effect of rectal heterogeneity on wall dose in high dose rate brachytherapy. *Med Phys* 2009; 36: 224-232.
19. Carrara M, Cutajar D, Alnaghy S et al. Semiconductor real-time quality assurance dosimetry in brachytherapy. *Brachytherapy* 2018; 17: 133-145.
20. Cygler JE, Saoudi A, Perry G et al. Feasibility study of using MOSFET detectors for in vivo dosimetry during permanent low dose-rate prostate implants. *Radiother Oncol* 2006; 80: 296-301.
21. Safigholi H, Meigooni AS, Song WY. Comparison of 192Ir, 169Yb, and 60Co high-dose rate brachytherapy sources for skin cancer treatment. *Med Phys* 2017; 44: 4426-4436.
22. Kron T, Duggan L, Smith T et al. Dose response of various radiation detectors to synchrotron radiation. *Phys Med Biol* 1998; 43: 3235-3259.
23. Davis SD, Ross CK, Mobit PM et al. The response of lif thermoluminescence dosimeters to photon beams in the energy range from 30 kV X-rays to Co-60 gamma rays. *Radiat Prot Dosimetry* 2003; 106: 33-43.
24. Haworth A, Butler DJ, Wilfert L et al. Comparison of TLD calibration methods for 192Ir dosimetry. *J Appl Clin Med Phys* 2013; 14: 4037.

25. Garcia-Martinez T, Chan JP, Perez-Calatayud J et al. Dosimetric characteristics of a new unit for electronic skin brachytherapy. *J Contemp Brachytherapy* 2014; 6: 45-53.

26. Kry SF, Smith SA, Weathers R et al. Skin dose during radiotherapy: a summary and general estimation technique. *J Appl Clin Med Phys* 2012; 13: 3734.

27. Panettierei V, Barsoum P, Westermark M et al. AAA and PBC calculation accuracy in the surface build-up region in tangential beam treatments. Phantom and breast case study with the Monte Carlo code PENELOPE. *Radiother Oncol* 2009; 93: 94-101.

28. Court LE, Tishler RB, Xiang H et al. Experimental evaluation of the accuracy of skin dose calculation for a commercial treatment planning system. *J Appl Clin Med Phys* 2008; 9: 29-35.

29. Granero D, Perez-Catalayud J, Vijande J et al. Limitation of the TG-43 formalism for skin high-dose-rate brachytherapy dose calculations. *Med Phys* 2014; 41: 0201703.

30. Boman EL, Satherley T, Schleich N et al. The validity of Acuros BV and TG-43 for high-dose-rate brachytherapy superficial mold treatments. *Brachytherapy* 2017; 16: 1280-1288.

31. Niu H, Hsi WC, Chu JC et al. Dosimetric characteristics of the Leipzig surface applicators used in the high dose rate brachy radiotherapy. *Med Phys* 2004; 31: 3372-3377.

32. Persson M, Nilsson J, Tedgren AC. Experience of using MOSFET detectors for dose verification measurements in an end-to-end 192Ir brachytherapy quality assurance system. *Brachytherapy* 2018; 17: 227-233.

33. Melchert C, Soror T, Kovács G. Quality assurance during interstitial brachytherapy: in vivo dosimetry using MOSFET dosimeters. *J Contemp Brachytherapy* 2018; 10: 232-237.

34. Roue A, Venselaar JLM, Ferreira IH et al. Development of a TLD mailed system for remote dosimetry audit for 192Ir HDR and PDR sources. *Radiother Oncol* 2007; 83: 86-93.